Coexistence of apoptosis, pyroptosis, and necroptosis pathways in Celiac Disease

Ruera Carolina N[1], Perez Federico[1], Iribarren María Luz[1], Guzman Luciana[2], Menendez Lorena[2], Garbi Laura[3], and Chirdo Fernando G[1*]

[1] Instituto de Estudios Inmunológicos y Fisiopatológicos (IIFP). (UNLP-CONICET-CIC) Facultad de Ciencias Exactas. Universidad Nacional de La Plata. La Plata. Argentina. [2] Servicio de Gastroenterología Hospital de Niños "Sor María Ludovica". La Plata. Argentina. [3] Servicio de Gastroenterología. Hospital San Martin. La Plata. Argentina

*Correspondence: fchirdo@biol.unlp.edu.ar

Abbreviations

CD: Celiac disease

DAMPs: Damage-associated molecular patterns

GSDMD: Gasdermin D

IBD: Inflammatory bowel disease

IEC: Intestinal epithelial cells

IELs: Intraepithelial lymphocytes

LP: Lamina propria

MFI: Mean fluorescence intensity

NC: Non-celiac

RCD: Regulated cell death

Abstract: Usually, the massive elimination of cells under steady-state conditions occurs by apoptosis, which is also acknowledged to explain the loss of enterocytes in the small intestine of celiac disease (CD) patients. However, little is known about the role of proinflammatory cell death pathways in CD. Here we have used confocal microscopy, Western blot, and RT-qPCR analysis to assess the presence of regulated cell death (RCD) pathways in the duodenum of CD patients. We found an increased number of dead ($TUNEL^+$) cells in the *lamina propria* of small intestine of CD patients, most of them plasma cells ($CD138^+$). Many dying cells expressed FAS and were in close contact with $CD3^+$ T cells. Caspase-8 and caspase-3 expression was increased in CD, confirming the activation of apoptosis. In parallel, caspase-1, IL-1β, and GSDMD were increased in CD samples indicating the presence of inflammasome-dependent pyroptosis. Necroptosis was also present, as shown by the increase of RIPK3 and phosphorylate MLKL (p-MLKL). Analysis of published databases confirmed that CD has an increased expression of RCD-related genes. Together these results reveal that CD is characterized by cell death of different kinds. In particular, the presence of proinflammatory cell death pathways may contribute to mucosal damage.

Keywords: Regulated cell death; small intestine; Celiac Disease, inflammation, intestinal epithelium, apoptosis, pyroptosis, necroptosis

Graphical_Abstract

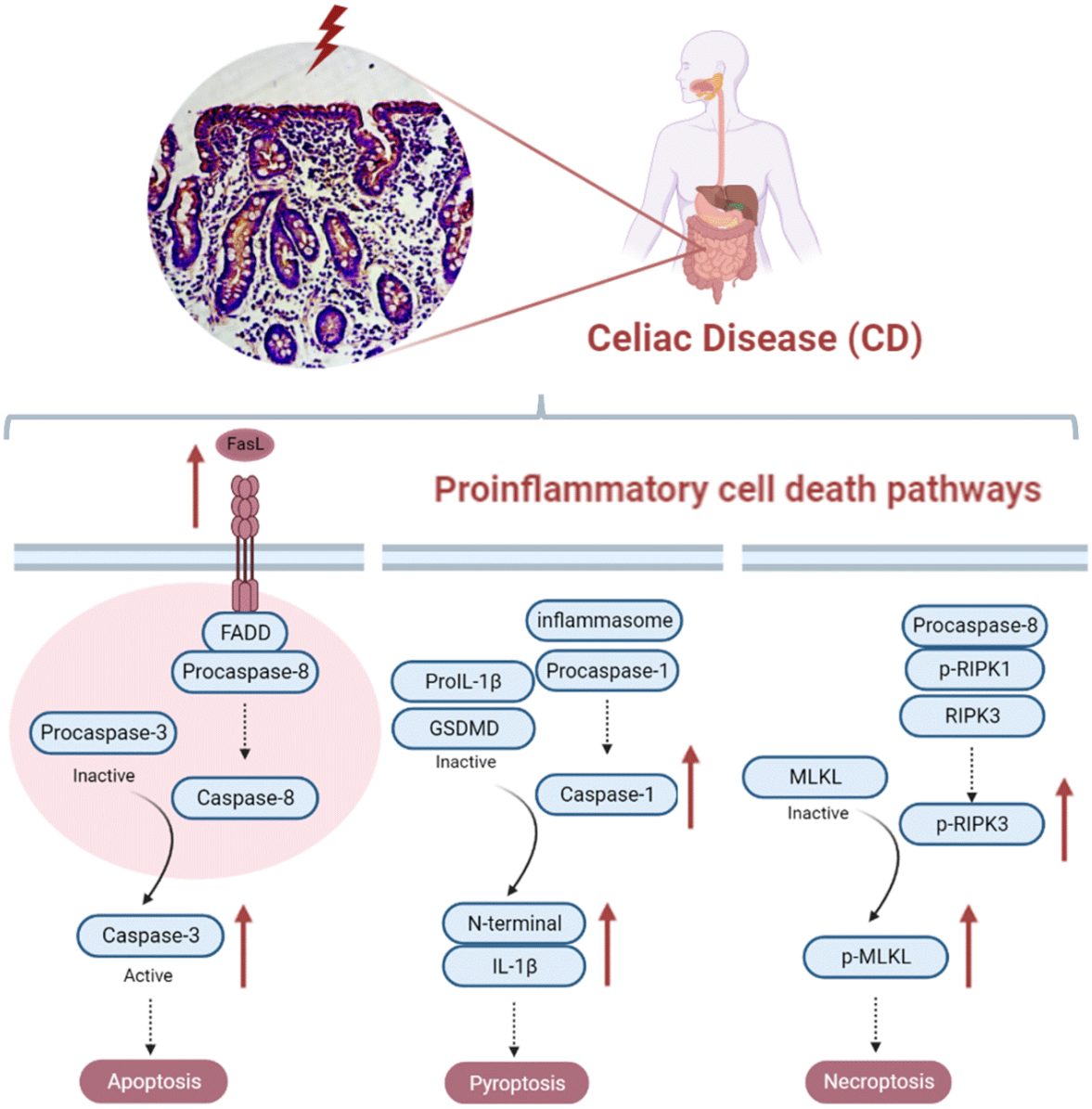

1. Introduction

Cell death is a constant feature of the intestinal mucosa under both physiological and pathological conditions and it has to be regulated carefully to avoid damage to the epithelial barrier. Apoptosis, the immunologically silent cell death program, guarantees the clearance of a massive number of dead cells without inflammation. Shedding of enterocytes takes place by a particular kind of apoptotic cell death, called anoikis, that occurs when epithelial cells lose the extracellular matrix protein-dependent communication that anchors them to the basal membrane. The dying cells are rapidly extruded from the epithelial layer by neighboring enterocytes and this process avoids the formation of gaps in the epithelium, allowing barrier integrity to be maintained [1,2].

Celiac disease (CD) is a chronic inflammatory enteropathy of the small intestine, that develops in genetically predisposed individuals as a consequence of an immune response to peptides from wheat, barley, and rye. It is driven by IFNγ produced by gluten-specific $CD4^+$ Th1 cells, accompanied by high levels of type I IFNs, IL-15, and IL-18 [3,4]. Together these mediators cause mucosal pathology, in part by stimulating the cytotoxic activity of $CD8^+$ T lymphocytes, γ/δ T cells, and NK cells which can induce apoptosis of enterocytes via FAS/FASL axis and release of perforin/granzyme B [5–9]. Some of the γ/δ T cells IELs play a regulatory function on T cell response but these populations are replaced by a particular subset of $V\delta1^+$ IELs secretes IFNγ contributing to epithelial damage in active CD [10].

While the participation of apoptosis in villous atrophy in CD has been studied [5,6,11,12], less is known about the potential role of proinflammatory cell death pathways such as pyroptosis. We showed that gliadin peptides, part of the gluten-derived peptides, are able to induce inflammasome activation *in vitro* and a mouse model of enteropathy. Several studies [13–17] reported that gliadin peptides induced inflammasome activation in peripheral blood mononuclear cells from CD patients, but activation of this cell death pathway was not assessed in the duodenum of CD patients. Necroptosis, another kind of proinflammatory RCD, was observed in inflamed ileum and colon samples of patients with Crohn's disease [18]. In contrast to apoptosis, pyroptosis, and necroptosis are lytic cell death programs that release cellular components and damage-associated molecular patterns (DAMPs), resulting in inflammation. In the intestine, this can lead to damage to the barrier and excessive translocation of macromolecules and components of the microbiota from the lumen [18]. Uncontrolled passage of this kind can initiate or sustain the chronic inflammation associated with intestinal disorders. However, these inflammatory forms of cell death have not been assessed in CD and here we report the presence of apoptosis, pyroptosis, and necroptosis in the duodenum of patients with untreated CD.

2. Materials and methods

2.1 Patients

Duodenal biopsies were collected from active celiac disease patients (ACD) and non-celiac (NC) individuals during the routine protocol for CD diagnosis in the Gastroenterology Units of the Hospital Sor María Ludovica, La Plata (pediatric patients) and Hospital San Martin, La Plata (adult patients).

Duodenal samples were collected from a total of 55 patients, in the period between 2017 and 2021. CD diagnosis was based on a positive serology (anti-transglutaminase-2, anti-deamidated gliadin peptides, and anti-endomysial antibodies) test and confirmed by duodenal biopsies assessed by a specialized pathologist. In this study, 15 patients were adults with an average age of 56.1 years, 12 were women, and 3 were men. Of them, 12 presented normal histology and serology, and 3 total villous atrophy. The remaining 40, were children with an average age of 7 years, 29 being females and 11 males. 14 presented normal histology, 22 total atrophy, and 4 partial villous atrophy. CD was diagnosed in 29 patients. The 26 individuals in the control group (NC) were subjected to endoscopy for reasons other than CD (mainly dyspepsia) and all were negative for serological or histological

evidence of CD. Once collected biopsies samples were processed for histology or immediately frozen and stored at -80°C until analysis by Western blot or RT-PCR.

2.2 Ethics statement

Informed consent was obtained from all subjects involved in the study. The study was approved by the Ethical Committees of both Public Health Institutions and performed according to human experimental guidelines. The clinical investigation was conducted according to the Declaration of Helsinki principles with participants identified only by number.

2.3 Western blot analysis

Duodenal biopsies were frozen on dry ice immediately after collection and were resuspended in cell lysis buffer (0.93 M Hepes, pH 7.9, 0.5 M EDTA, 1 M KCl, 1% v/v Nonidet P40), supplemented with Complete™ Protease Inhibitor Cocktail (Roche, Castle Hill, NSW, Australia). The total protein level was assessed using the bicinchoninic acid method (BCA, Pierce Laboratories, Rockford, IL) following the manufacturer's instructions. Protein samples (30 µg/lane) were separated by sodium dodecyl sulfate-polyacrylamide gel electrophoresis on 12.5% gels with a mini-Protean II Hercules (Bio-Rad, USA) and transferred onto 45 µm pore size nitrocellulose membranes (45-004-113, GE Healthcare, USA). The membranes were blocked with 5% w/v fat-free dry milk in TBST (tris-buffered saline, 0.1% v/v Tween 20, pH 8) at 37°C for 1 h and incubated at 4°C overnight with the following primary antibodies: anti-caspase-3 (1/500, Cell Signaling Technology Cat# 9662, RRID: AB_331439, USA), anti-caspase-8 (1/700, Novus Cat# NB100-56116, RRID: AB_837874, USA), anti-caspase-1 (1/150, Santa Cruz Biotechnology Cat# sc-56036, RRID: AB_781816, USA), anti-GSDMD (1/100, ab225867, Abcam, USA), anti-IL-1β (1/100, Thermo Fisher Scientific Cat# P420B, RRID: AB_223478, USA), anti-RIPK3 (1/80, Abcam Cat# ab56164, RRID: AB_2178667, USA), anti-β-actin (1/2000, Abcam Cat# ab8227, RRID: AB_2305186, USA). After washing with TBST, membranes were incubated with horseradish peroxidase (HRP)-conjugated secondary goat anti-rabbit antibody (1/2000, Bio-Rad Cat# 170-6515, RRID: AB_11125142), or horseradish peroxidase (HRP)-conjugated secondary anti-mouse antibody (1/3000, Abcam Cat# ab6789, RRID: AB_955439, USA) at 37°C for 1 h, and visualized using the enhanced chemiluminescent reagent (GE Healthcare). The relative levels of the target protein were determined using Image-J software. In all cases, β-actin was used as a loading control. In some assays, due to limitations in the duodenal samples, a harsh stripping was performed. After the first development, the membrane was incubated at 50°C for 30 min under agitation with the buffer (Tris-HCl 62,5Mm, SDS 2%, β-mercaptoethanol 100mM. pH6,7). Then was washed under a running water tap for 1 min, followed by 5 min in TBST, and blocked again for the determination of a new protein.

2.4 TUNEL reaction

5 µm paraffin-embedded sections were deparaffinized and rehydrated in distilled water and treated with the DeadEnd™ Fluorometric TUNEL system (G3250, Promega, Madison USA) according to the manufacturer's instructions. Nuclear staining was assessed using IP or DAPI (ThermoFisher, # D3571, RRID: AB_2307445, USA) at 1µg/ml and TUNEL$^+$ cells were identified by immunofluorescence as described above using primary antibodies: anti-CD45 (1/50, Dako Cat# A0452, RRID: AB_2335677, USA), anti-CD3 (1/50, Santa Cruz Biotechnology Cat# sc-1178, RRID: AB_627074, USA), anti-CD20 (1/50, Thermo Fisher Scientific Cat# 17-0209-42, RRID: AB_10670628, USA), anti-CD64 (1/50, Santa Cruz Biotechnology Cat# sc-1184, RRID: AB_627153, USA) anti-CD138(1/30, Dako Cat# M7228, RRID:

AB_2254116, USA), anti-CD95 (1/50, BV421, BD, USA). After mounting (S3023, Dako Cytomation, USA), sections were visualized using a Nikon Eclipse Ti fluorescence microscope (light source: X-Cites Series 120 Q). The images were obtained with a Nikon camera (Nikon Digital Sight DS Ri1), using the NIS-Elements software, and cells were counted using Image-J software, calibrated to allow for measurement of the area of randomly selected *lamina propria* regions and the results were expressed as the number of $TUNEL^+$ cells/μm^2 of *lamina propria*.

2.5 Immunofluorescent microscopy

Duodenal samples were fixed with 4% w/v formalin for 24 h at room temperature. Samples were dehydrated and embedded in paraffin, and sections of 5 µm were deparaffinized and rehydrated in distilled water. Antigen retrieval was performed by heat treatment in sodium citrate 10 Mm, pH 6. The tissues samples were blocked using horse serum at 5% in PBS for 1 h at room temperature in a humidified chamber, and then incubated with primary antibodies: anti-caspase-3 (1/100, Cell Signaling Technology Cat# 9662, R RID: AB_331439, USA), anti-caspase-8 (1/100, Novus Cat# NB100-56116, RRID: AB_837874, USA), anti-caspase-1 (1/100, Santa Cruz Biotechnology Cat# sc-56036, RRID: AB_781816, USA), anti-RIPK3 (1/30, Abcam Cat# ab56164, RRID: AB_2178667, USA), anti-GSDMD (1/80, ab225867, Abcam, USA), anti-IL-1β (1/100, Thermo Fisher Scientific Cat# P420B, RRID: AB_223478, USA). After overnight incubation, the samples were washed with PBS buffer and then incubated with secondary antibodies: anti-IgG (Mouse)-Alexa Fluor 647 (Abcam, Cat# ab150107, USA), anti-IgG (Rabbit)-Alexa Fluor 647 (Abcam, Cat# ab150075, RRID: AB_2752244, USA). For nuclear staining, we used DAPI (ThermoFisher, Cat# D3571, RRID: AB_2307445, USA) at 1 µg/ml. After mounting (S3023, Dako Cytomation, USA), samples were visualized using a TCS SP5 confocal microscope (Leica) and images were analyzed using Leica LAS AF software and Image-J software. In all the images from the same staining procedure, the fluorescence staining intensity was obtained under the same acquisition parameters (light intensity, sensor gain, and exposure time).

2.6 Image analysis

The Image-J free software was used to perform the image analysis. To quantify the mean fluorescence intensity (MFI) or the cell counting, manual sectioning of the images was performed with automatic thresholding (Image-J "Default" method) to determine the total area of each section. This procedure provided a good separation between histologically different regions, such as epithelium and lamina propria from "black" or empty spaces between cells and staining artifacts. The cell counting was performed manually for each region of interest. Meanwhile, we obtained the MFI by the Image-J software for the same regions from images obtained with the same acquisition parameters. A variable number of images per sample was obtained due to differences in available tissue with adequate histology and regions without artifacts. To collect representative data, we processed a minimum of five and a maximum of ten fields per sample using a 20X or 40X objective.

2.7 Gene expression analysis

Duodenal samples from human patients were obtained in RNA Later Solution (Biogenex) and stored at -80ºC. Total RNA was isolated with an RNA Spin Mini kit (GE Healthcare, USA) and reverse transcription was performed using 1µg of total RNA using MML-V polymerase and random primers (Molecular Probes Inc., Invitrogen, Carlsbad, CA, USA). Real-time PCR (qPCR) analysis was performed using an IQ5-Cycler (Bio-Rad) with the SYBR Green Supermix (Invitrogen, 11761-100, USA) and the primers shown in **Table 1** (Genbiotech, Buenos Aires, Argentina). *EEF1A1* transcript was used as a

housekeeping gene and the threshold cycle was used to indicate the relative expression level. All cycles were 95°C for 10 min and 50 cycles of 95°C for 10 s, 60°C for 15 s, and 72°C for 45 s.

Table 1. Primers sequences

Gene	Forward primer	Reverse primer
EEF1A1	TCGGGCAAGTCCACCACTAC	CCAAGACCCAGGCATACTTGA
ZBP1	GCAAACTCCGAAGCCATCCAGA	CCAAGTTGAGGAATCACCTGGTG
NLRP3	GGACTGAAGCACCTGTTGTGCA	TCCTGAGTCTCCCAAGGCATTC
AIM2	GCTGCACCAAAAGTCTCTCCTC	CTGCTTGCCTTCTTGGGTCTCA
GSDMD	ATGAGGTGCCTCCACAACTTCC	CCAGTTCCTTGGAGATGGTCTC
MLKL	TCACACTTGGCAAGCGCATGGT	GTAGCCTTGAGTTACCAGGAAGT
IL-1B	AATCTGTACCTGTCCTGCGTGTT	TGGGTAATTTTTGGGATCTACACTCT

2.8 Transcriptomic data analysis of differentially expressed genes related to regulated cell death pathways from public databases

The GSE164883 public database was used to analyze differentially expressed genes (DEGs) related to RCD pathways in samples from CD patients [20]. As described in the original paper, this database was made up of microarray analysis of total RNA from duodenal mucosa of 24 CD patients and 21 non-CD patients as controls. Here, the whole analysis was performed on the published count gene expression matrix considering the associated relevant metadata. After computing a standard normalization, poorly expressed genes were eliminated using the edgeR (3.38.4) package and DEGs were identified using the R package limma (v3.52.3) as described previously [21]. The DEGs were used to perform enrichment analysis and GSEA analysis for REACTOME and GO database pathways related to RCDs. The analysis was computed with ReactomePA (v 1.40.0) and ClusterProfiler (v 4.4.4) packages in R (v 4.2.1) [22]. P-values were adjusted by the Benjamini-Hochberg (BH) method.

DEG analysis was also performed on the published gene count matrix from the EGAS00001004623 database which contains 3,251 sorted plasma cells with quality-checked gene reads from 15 patients with ACD, 26 CD patients on gluten-free diets (treated CD - TCD), and 13 non-CD controls [23]. Quality control and data normalization were performed using the parameters described in the original publication and DEGs were computed using the scanpy toolkit (v1.9.1) using the corrected gene expression matrix as input and a Wilcoxon rank-sum test with the BH correction method for multiple testing [23]. The parameters for the selection of DEGs were log2FC > 0.25 and adjusted P-value <0.01. A heatmap for selected DEGs related to RCD pathways was generated using

the “sc.pl.matrixplot” function of the scanpy toolkit (v1.9.1), with the DEGs being sorted by their fold change in descending order.

2.9 Statistical Analysis

Statistical analysis was performed using Graph-Pad Prism software (San Diego, United States). When two groups were compared, an unpaired Student's t-test was used with eventual Welch correction for populations with different SD. P-values <0.05 was considered significant. Data are displayed as means ± 1 SEM.

3. Results

3.1 Increased cell death in the duodenal mucosa of patients with active CD

To assess cell death in CD, we first used the TUNEL reaction to determine the total number of dead cells in sections of duodenal biopsies from untreated CD patients (ACD) and non-CD (NC) controls. As shown in **Figure 1,** a higher number of $TUNEL^+$ cells was found in mucosa from CD patients when compared with non-CD samples. Strikingly, most dead cells were found scattered in *lamina propria* (LP) (**Figure 1.A**) and rarely in the epithelium (**Suppl. Figure 1.B**). This may be because the TUNEL reaction detects the late stages in the cell death process and so may not identify dying enterocytes that are rapidly extruded from the epithelial layer.

CD45 expression was observed in the majority of $TUNEL^+$ cells in the LP of CD patients. These cells were $CD138^+$ plasma cells (73%) and the remainder being $CD20^+$ B lymphocytes (27%), $CD64^+$ monocytes/macrophages/neutrophils (8%), and $CD3^+$ T lymphocytes (5%) (**Figures 2.A-C, Suppl. Figure 1.C**). A similar distribution was found in the samples from NC patients (**Suppl. Figure 1.D)**. Most $TUNEL^+$ cells in ACD also expressed CD95 (Fas) and were found in close contact with $CD3^+$ T cells, phenomenon not observed in control patients (**Figure 2.C, Suppl. Figure 1.D**), suggesting a potential role of T cell-mediated cytotoxicity mediated by the Fas/FasL axis in ACD.

3.2 Cleaved caspase-8 and caspase-3 are increased in the duodenal tissue of ACD patients

As some of the dying cells expressed CD95 (Fas) in active CD and the extrinsic pathway of apoptosis has been identified as the most common mechanism of cell death in the small intestine in untreated CD [5,6], we next assessed whether other components of this pathway were activated in this tissue.

Indirect immunofluorescence analysis of sections of duodenal biopsies showed that caspase-8 and caspase-3 expression was restricted to epithelial cells at the tips of the villi in control samples, consistent with the physiological process of enterocyte turnover, (**Suppl. Figure 2**). In contrast, there was increased expression of caspase-8 and caspase-3 both in the epithelium and LP of untreated CD patients compared with control LP (**Figure 3.A)**. Quantitative analysis of fluorescence intensity showed significantly higher expression in ACD versus NC samples and there was also increased expression of cleaved caspase-3 in the epithelium of CD samples (**Suppl. Figure 2.C**). Western blot

analysis confirmed that the full-length forms of caspase-8 and caspase-3 were increased in ACD samples compared with controls and there was a significant increase in the cleaved caspase:procaspase ratio for both caspases in ACD mucosa (**Figure 3.B-C**). Active caspase-8 and caspase-3 were also increased relative to the reference protein (β-actin) in ACD, indicating that both proteins increased their expression, as well as their activation being increased (not shown).

These findings show that the extrinsic apoptosis pathway is activated in the small intestine of CD patients.

3.3 Pyroptosis is present in the duodenal mucosa of ACD patients

To assess whether pro-inflammatory cell death pathways are also active in CD, the activation of key downstream factors of inflammasome activation and pyroptosis (caspase-1, GSDMD, and IL-1β) were studied. Immunofluorescence analysis showed a significant increase in the expression of all these molecules in the duodenal mucosa of untreated CD compared with controls (**Figure 4.A**) Interestingly, there was a particularly strong expression of caspase-1 in the crypts of CD samples (**Suppl. Figure 3.A**). Western blot analysis confirmed there was increased expression of active (cleaved) caspase-1 relative to pro-caspase-1 in active CD, as well as higher levels of the active N-terminal form of GSDMD and active IL-1β (**Figure 4.B-C**). Accordingly, an increased expression of IL-1β and GSDMD mRNA in CD was observed (**Suppl. Figure 3.B-C**). This evidences that the inflammasome pathway is active in CD. In addition, we also found an increased mRNA expression of the inflammasome components, NLRP3 and AIM2, in CD versus control samples (**Suppl. Figure 3.D-E**).

3.4 Expression of RIPK3 and MLKL, members of the necroptosis pathway, is increased in ACD

Necroptosis is an additional form of inflammatory cell death and to assess whether this was also active in CD, we examined the expression of RIPK3 and p-MLKL, two essential components of this pathway.

Indirect immunofluorescence showed increased RIPK3 expression in the surface epithelium and crypts, as well as in some LP cells in untreated CD (**Figure 5.A**) and a trend to higher values by Western blot analysis, (**Figure 5.B**). There were also higher levels of MLKL mRNA in CD patients (**Figure 5.E**) and Western blot analysis showed a significant increase in the expression of the biologically active, pore-forming form of p-MLKL in these samples (**Figure 5.C**). The p-MLKL$^+$ cells were scattered in the LP and epithelium. Most of the epithelial p-MLKL$^+$ cells were positive for the DEF5A marker (Paneth cells), while some LP cells were CD3$^+$ T lymphocytes (**Figure 5.D**).

Z-DNA-binding protein 1 (ZBP1) has recently been revealed to be involved in many forms of RCD, including apoptosis, pyroptosis, and necroptosis, and we, therefore, explored its expression as an additional measure of these processes in CD. RT-qPCR analysis revealed that ZBP1 transcription was increased in the duodenum of CD patients compared with controls (**Figure 5.F**).

3.5 Regulated cell death gene signatures in celiac disease

To explore the presence of RCD pathways in CD through a different strategy, we took advantage of published public databases from CD and control populations, and different RCD-related gene lists from curated databases. This strategy allowed us to search in the whole transcriptome of duodenal mucosal biopsies of CD patients the upregulation of key markers of different RCD

pathways. The differentially expressed gene analysis of the public database obtained from the whole duodenal mucosa of 24 CD patients and 21 non-CD controls (GSE164883) [20] showed significant upregulation of several genes associated with apoptosis, necroptosis, and pyroptosis, such as FAS, BAK1, CASP3, CASP1, MLKL, ZBP1, GSDMD, and GSDMB (**Figure 6.A**). To further analyze the involvement of concrete RCD pathways in the duodenum of CD patients, we performed a gene set enrichment analysis (GSEA) using gene lists from popular curated databases (GO and REACTOME). The corresponding results demonstrate that several DEGs found in the CD population associate apoptotic and necroptotic pathways with the CD population (**Suppl. Figure 4**). Remarkably, all the associated pathways have a positive NES, meaning the overrepresented genes are upregulated. These findings support the activation of RCD pathways in CD enteropathy.

As a high proportion of the TUNEL$^+$ cells found in active CD were CD138$^+$ plasma cells, we investigated the expression of RCD pathway-related genes in these cells specifically. To do this, we mined a recently published single-cell RNAseq database of plasma cells from the duodenum of ACD, TCD, and controls (EGAS00001004623) [23]. This showed increased expression of CASP3, BAK1, and MLKL by plasma cells of CD patients, suggesting that apoptosis and necroptosis may explain the death of plasma cells we observed (**Figure 6.B**). We also found opposite results in the expression of some genes (GADD45A, BCL2, DDIT2, HSP90AA1) when compared with the former analysis in the bulk tissue. These results might represent differences in the DEGs between plasma cells and other cell populations.

4. Discussion

In this study, we showed the presence of the active forms of key players of apoptosis, pyroptosis, and necroptosis in the proximal small intestine of untreated CD patients. An increased number of dead cells in *lamina propria* evidences the exacerbation of RCD in tissue with chronic damage. Caspase-8 and -3 were overexpressed together with an increase in their biologically active forms, supporting a role in apoptosis in CD. In addition, while increases in N-term GSDMD fragments and IL-1β indicate local inflammasome activation, expression of RIPK3 and active MLKL suggest the activation of the necroptosis pathway in CD.

That apoptosis is the main RCD pathway in the small intestine in CD is also supported by the expression of caspase-8 and caspase-3 observed by immunofluorescence in intestinal epithelial cells, while cleaved/ full versions ratio of these caspases was markedly increased in the duodenum of CD patients. Since the extrusion of enterocytes can be completed in minutes [24], dead enterocytes were rarely found by TUNEL reaction which detects late stages of cell death. Similarly, caspase-3$^+$ cells were occasionally found as unique events in the epithelium, particularly in the upper part of the villi in CD samples, indicating the high rate of enterocyte death and extrusion in the tip of the villi [25].

Similar findings were reported by immunohistochemistry in previous studies [11]. Together these findings confirmed that activation of apoptosis may contribute to cell death in CD.

In contrast to the epithelium, TUNEL$^+$ cells could be detected in the normal LP and the numbers of TUNEL$^+$ LP cells were greatly increased in CD patients, confirming previous work [5,12] Apoptotic cells in the LP included cells expressing the Fas death receptor. Similarly, Maiuri L et al. reported Fas expressing mononuclear cells in the LP after *in vitro* gluten challenge of CD biopsies [7]. We found CD3$^+$ T lymphocytes close to dead cells in celiac LP, which could indicate a role for activated, FasL-expressing T cells in causing apoptosis of LP cells under these conditions. However, we were unable to confirm this idea by immunofluorescence and we cannot exclude a role for other mechanisms that could promote cell death such as IL-15, type I IFNs, IFNγ, granzyme and perforin, all of which are known to be enhanced in CD [26].

We have already shown that CXCL10, overproduced in the duodenum of untreated CD patients, is a critical signal for the recruitment of plasma cells. Interestingly, CXCL10 is produced by

lamina propria CD138$^+$ cells of untreated CD patients [27]. CXCR3/CXCL10 axis is overexpressed in the duodenum of CD patients and may work as a stimulatory circuit to maintain a high number of plasma cells in this tissue under a chronic inflammatory response. Here, we found that most of the TUNEL$^+$ cells were CD138$^+$ plasma cells, which is the major cell population in the small intestine lamina propria, and their numbers are markedly increased in CD. These immunofluorescence findings were supported by the transcriptional analysis we performed on the public database of plasma cells sorted from CD mucosa, where several genes associated with cell death were amongst the DEGs identified [23]. As many of the plasma cells in untreated CD are short-lived, particularly those called disease-specific producing anti-TG2 or anti-deamidated gluten peptides antibodies, it would seem likely that there is constant cell death amongst this population, an idea which would be consistent with our findings. Indeed, this recent work has shown that the DEGs expressed by short-lived plasma cells in celiac mucosa include genes from RCD pathways, as well as XBP1, an essential factor for plasma cell differentiation. However, as XBP1 is also an important component of the ER stress response [28], these findings may reflect the high rate of immunoglobulin synthesis which occurs in LP plasma cells in CD, leading to ER stress and high cell death in LP plasma cells.

Unlike apoptosis, cell death pathways such as pyroptosis and necroptosis lead to the production of inflammatory mediators such as IL-1β, IL-33, and HMGB1, all of which can enhance tissue damage [29] and have been detected in the serum or mucosa in active CD (30-34). However, these death processes have not been described previously in celiac mucosa. Here we found an increase in the active forms of caspase-1, IL-1β, and GSDMD in active CD, indicating activation of the inflammasome pathway leading to pyroptotic cell death.

Supporting the presence of inflammasome activation, immunofluorescence, and Western blotting revealed increased levels of IL-1β in the duodenal mucosa of CD patients, extending the finding of higher serum levels of this cytokine in CD patients [33]. Previous studies have reported that gliadin-derived peptides can induce caspase-1-dependent release of IL-1β by PBMC of CD patients [13] and we have shown that the gliadin peptide, p31-43, can drive inflammasome activation *in vitro* assessed by ASC speck formation assay [15,17,35]. Furthermore, oral administration of p31-43 causes mucosal damage in the normal mouse small intestine, associated with the local production of the active forms of caspase-1, IL-1β, and GSDMD [16]. Blockade of IL-1β using a specific monoclonal antibody inhibited the induction of intestinal mucosal damage and apoptosis in this model of sterile inflammation in the small intestine, highlighting the role of IL-1β in driving RCD pathways and tissue damage [36]. p31-43 also induces increased production of IL-1β by intestinal organoids from active CD mucosa [37]. Together these results indicate that inflammasome activation occurs in the small intestine during CD and suggest that gliadin peptides can be in part, responsible for this process. We found here that the NLRP3 and AIM2 components of the inflammasome were upregulated in CD mucosa. Both inflammasomes can be upregulated by an environment rich in mediators promoting NF-kB activation or type I IFNs signaling, respectively [38]. However, the exact nature of the active inflammasome in this condition remains to be identified. It is also not clear what role the inflammasome might play in the pathogenesis of enteropathy in CD, but the release of its end products (IL-1β and IL-18) and DAMPs may enhance intestinal inflammation and epithelial damage.

Necroptosis is a further form of inflammatory cell death that occurs when apoptosis is inhibited in presence of signals that normally induce apoptosis by mediators such as TNFα or Fas and is driven by activation of RIPK3 and MLKL [39]. Here we show that there was increased expression of RIPK3 and p-MLKL in celiac mucosa, with p-MLKL being detectable in villus and crypt epithelium, as well as in cells in the LP. The p-MLKL$^+$ cells in LP were identified as CD3$^+$ T cells in untreated CD. A similar expansion of MLKL-expressing T cells has been reported in ulcerative colitis mucosa [40], again suggesting the activation of particular cell death processes in chronic inflammatory diseases of the intestine. Particularly, when caspase-8 was inhibited, regulatory T cells were more sensitive to necroptosis in the presence of type I IFNs, IL-12, or IL-18, and signals driven by TNFα or FASL [41].

We could not determine the phenotype of $CD3^+$ T cells in our study, but inflammatory mediators, TNFα or FASL are present in CD mucosa and this microenvironment may affect differentially to the distinct T cell types.

Necroptosis can be induced by TNFα and FasL and these signals can be potentiated in the presence of IFNγ. All these mediators are overexpressed in CD, particularly the synergistic effect of IFNγ and TNFα upregulates transglutaminase 2 in the mucosa of CD patients [42]. The combination of IFNγ and TNFα may also induce a caspase-8-JAK1/2-STAT1-dependent intestinal epithelial cell death via non-canonical TNFR signaling [43]. Interestingly, the p-$MLKL^+$ cells at the base of crypts could be identified as α5 $defensin^+$ Paneth cells, whose numbers have been reported to be reduced in untreated CD patients [44]. $RIPK3^+$ Paneth cells have also been found in the ileum of Crohn's disease patients [39], suggesting that chronic inflammation may have a selective ability to promote necroptosis in these cells.

The interconnection between apoptosis, pyroptosis, and necroptosis led to the proposal of the term PANoptosis [45]. ZBP1, a nucleic acid sensor, is a central piece in the regulation of cell death and may participate in intestinal epithelial cell death, leading to ileitis or colitis in mice depending on the level of its expression [46]. Here, the study of the proximal small intestine from CD samples showed upregulation of ZBP1 in CD samples. Interferon regulatory factor 1 (IRF1), another factor involved in all three death processes in the colon [47], is also upregulated in Celiac mucosa [48]. Together these findings, where caspase-8 appears as a key player, unveil the complexity of simultaneous mechanisms leading to cell death through different pathways.

In the analysis of the public database (GSE164883) from duodenal samples of CD patients and non-CD controls [20], key genes involved in apoptosis, pyroptosis, and necroptosis were found differentially expressed. Transcriptome from the duodenum of CD shows upregulation of *CASP3, FAS, BAK1, GSDMD/B, CASP1, ZBP1,* and *MLKL* among others, suggesting that different cell death pathways are simultaneously active in the CD enteropathy. Also, GSEA analysis confirmed that up-regulated expression of overrepresented genes in CD patients is associated with RCD pathways. IFN pathways, strongly associated with apoptosis, pyroptosis, and necroptosis can be considered as one of the candidates linking these mechanisms.

Apoptosis, pyroptosis, and necroptosis share different elements and regulate each other, being a complex interconnected network, an outstanding finding from our study was that three distinct pathways of cell death were occurring in the mucosa of CD. This was confirmed by several different approaches, including immunofluorescence, Western blotting, RT-qPCR, and analysis of DEGs. While these effects may not be entirely unsurprising given the high levels of environmental stress, inflammatory cytokines such as IFNγ and TNFα, and rapid turnover of both epithelial and immune compartments seen in CD, the mechanisms responsible remain to be elucidated. This situation is similar in other autoimmune and inflammatory scenarios [49] in the gut, like Crohn's disease, where recently been shown that different IFNs might be responsible for inducing necroptosis in Paneth cells and apoptosis in IECs [50].

The field of regulated cell death is rapidly expanding. Ferroptosis, another RCD pathway, generated by an imbalance between oxidation and antioxidant mechanisms, has been also documented in the inflamed intestine in IBD patients and colitis mouse models [51]. Ferroptosis needs to be investigated in the proximal small intestine in the context of inflammation and celiac disease, but it is beyond the scope of this work.

Our study is based on the analysis of human duodenal samples, that focused on the investigation of three central cell death pathways. The rationale for selecting these pathways include their well described role in many different cell types and that they are tightly interconnected. Human ethics restrict the amount of tissue that can be obtained from patients,

which in our country is 1 biopsy for research purposes. Because endoscopic duodenal biopsies are small, this unfortunately limits the measurements that can be performed with this material. We acknowledge further characterization of additional types of cell death occurring in different cellular compartments of the gut in patients with celiac disease would be highly desirable. This will require new patient recruitment and sampling material during endoscopic procedures.

Our findings unveil that, in addition to the generally accepted notion that apoptosis is the predominant and immunologically silent cell death in CD, the highly inflammatory nature of lytic cell death pathways, necroptosis or pyroptosis, may take part in driving, expanding or in the chronic phase of CD.

5. Conclusion

In summary, a high number of dead cells were found in the duodenum of CD patients, with apoptosis, pyroptosis, and necroptosis appearing to occur in parallel. DAMPs released during proinflammatory cell death may play a role in the initial steps of the induction of mucosal damage and promote chronic disease.

References

1. Hall PA, Coates PJ, Ansari B, Hopwood D. Regulation of cell number in the mammalian gastrointestinal tract: The importance of apoptosis. *J Cell Sci*. 1994;107(12):3569-3577.
2. George T. Eisenhoffer, Patrick D. Loftus, Masaaki Yoshigi, Hideo Otsuna, Chi-Bin Chien, Paul A. Morcos and JR. Crowding induces live cell extrusion to maintain homeostatic cell numbers in epithelia. *Nature*. 2015;5(6):1-8. doi:10.1038/nature10999.Crowding
3. Abadie V, Sollid LM, Barreiro LB, Jabri B. Integration of genetic and immunological insights into a model of celiac disease pathogenesis. *Annu Rev Immunol*. 2011;29:493-525. doi:10.1146/annurev-immunol-040210-092915
4. Iversen R, Sollid LM. The Immunobiology and Pathogenesis of Celiac Disease. *Annu Rev Pathol*. Published online September 2022. doi:10.1146/annurev-pathmechdis-031521-032634
5. Di Sabatino A, Ciccocioppo R, D'Alò S, et al. Intraepithelial and lamina propria lymphocytes show distinct patterns of apoptosis whereas both populations are active in Fas based cytotoxicity in coeliac disease. Gut. 2001;49(3):380-386. doi:10.1136/gut.49.3.380
6. Ciccocioppo R, Di Sabatino A, Parroni R, et al. Increased enterocyte apoptosis and Fas-Fas ligand system in celiac disease. Am J Clin Pathol. 2001;115(4):494-503. doi:10.1309/UV54-BHP3-A66B-0QUD
7. Maiuri L, Ciacci C, Vacca L, et al. IL-15 drives the specific migration of CD94+ and TCR-γδ+ intraepithelial lymphocytes in organ cultures of treated celiac patients. Am J Gastroenterol. 2001;96(1):150-156. doi:10.1016/S0002-9270(00)02230-9
8. Meresse B, Chen Z, Ciszewski C, et al. Coordinated induction by IL15 of a TCR-independent NKG2D signaling pathway converts CTL into lymphokine-activated killer cells in celiac disease. Immunity. 2004;21(3):357-366. doi:10.1016/j.immuni.2004.06.020
9. Jarry A, Malard F, Bou-Hanna C, et al. Interferon-Alpha Promotes Th1 Response and Epithelial Apoptosis via Inflammasome Activation in Human Intestinal Mucosa. Cmgh. 2017;3(1):72-81. doi:10.1016/j.jcmgh.2016.09.007
10. Mayassi T, Ladell K, Gudjonson H, et al. Chronic Inflammation Permanently Reshapes Tissue-Resident Immunity in Celiac Disease. Cell. 2019;176(5):967-981.e19. doi:10.1016/j.cell.2018.12.039
11. Shalimar, Das P, Sreenivas V, Gupta SD, Panda SK, Makharia GK. Mechanism of villous atrophy in celiac disease: Role of apoptosis and epithelial regeneration. Arch Pathol Lab Med. 2013;137(9):1262-1269. doi:10.5858/arpa.2012-0354-OA
12. Moss SF, Attia L, Scholes J V., Walters JRF, Holt PR. Increased small intestinal apoptosis in coeliac disease. Gut. 1996;39(6):811-817. doi:10.1136/gut.39.6.811
13. Palová-Jelínková L, Dáňová K, Drašarová H, et al. Pepsin Digest of Wheat Gliadin Fraction Increases Production of IL-1β via TLR4/MyD88/TRIF/MAPK/NF-κB Signaling Pathway and an NLRP3 Inflammasome Activation. PLoS One. 2013;8(4). doi:10.1371/journal.pone.0062426
14. Araya RE, Castro MFG, Carasi P, et al. Mechanisms of innate immune activation by gluten peptide p31-43 in mice. Am J Physiol - Gastrointest Liver Physiol. 2016;311(1):G40-G49. doi:10.1152/ajpgi.00435.2015
15. Gómez Castro MF, Miculán E, Herrera MG, et al. P31-43 gliadin peptide forms oligomers and induces NLRP3 inflammasome/caspase 1-dependent mucosal damage in small intestine. Front Immunol. 2019;10(JAN):1-11. doi:10.3389/fimmu.2019.00031
16. Ruera CN, Miculán E, Pérez F, Ducca G, Carasi P, Chirdo FG. Sterile inflammation drives multiple programmed cell death pathways in the gut. J Leukoc Biol. 2021;109(1):211-221. doi:10.1002/JLB.3MA0820-660R
17. Chirdo FG, Auricchio S, Troncone R, Barone MV. The Gliadin P31–43 Peptide: Inducer of Multiple Proinflammatory Effects. Vol 358. 1st ed. Elsevier Inc.; 2021. doi:10.1016/bs.ircmb.2020.10.003
18. Pierdomenico M, Negroni A, Stronati L, et al. Necroptosis is active in children with inflammatory bowel disease and contributes to heighten intestinal inflammation. Am J Gastroenterol. 2014;109(2):279-287. doi:10.1038/ajg.2013.403
19. Perez F, Ruera CN, Miculan E, Carasi P, Chirdo FG. Programmed cell death in the small intestine: Implications for the pathogenesis of celiac disease. Int J Mol Sci. 2021;22(14). doi:10.3390/ijms22147426
20. Wolf J, Willscher E, Loeffler-Wirth H, et al. Deciphering the transcriptomic heterogeneity of duodenal coeliac disease biopsies. Int J Mol Sci. 2021;22(5):1-29. doi:10.3390/ijms22052551
21. Smyth GK, Ritchie ME, Law CW, et al. RNA-seq analysis is easy as 1-2-3 with limma, Glimma and edgeR. F1000Research. 2018;5:1-30. doi:10.12688/f1000research.9005.3
22. Yu G, He Q-Y. ReactomePA: an R/Bioconductor package for reactome pathway analysis and visualization. Mol Biosyst. 2016;12(2):477-479. doi:10.1039/c5mb00663e
23. Lindeman I, Zhou C, Eggesbø LM, et al. Longevity, clonal relationship, and transcriptional program of celiac disease–specific plasma cells. J Exp Med. 2021;218(2). doi:10.1084/JEM.20200852
24. Wang F, Wang F, Zou Z, Liu D, Wang J, Su Y. Active deformation of apoptotic intestinal epithelial cells with adhesion-restricted polarity contributes to apoptotic clearance. Lab Investig. 2011;91(3):462-471. doi:10.1038/labinvest.2010.182
25. Bullen TF, Forrest S, Campbell F, et al. Characterization of epithelial cell shedding from human small intestine. Lab Investig. 2006;86(10):1052-1063. doi:10.1038/labinvest.3700464
26. Sollid LM, Jabri B. Triggers and drivers of autoimmunity: Lessons from coeliac disease. Nat Rev Immunol. 2013;13(4):294-302. doi:10.1038/nri3407
27. Bondar C, Araya RE, Guzman L, Rua EC, Chopita N, Chirdo FG. Role of CXCR3/CXCL10 axis in immune cell recruitment into the small intestine in celiac disease. PLoS One. 2014;9(2). doi:10.1371/journal.pone.0089068

28. Gass JN, Gifford NM, Brewer JW. Activation of an unfolded protein response during differentiation of antibody-secreting B cells. J Biol Chem. 2002;277(50):49047-49054. doi:10.1074/jbc.M205011200
29. Kesavardhana S, Malireddi RKS, Kanneganti T-D. Caspases in Cell Death, Inflammation, and Pyroptosis. Annu Rev Immunol. 2020;38(1):567-595. doi:10.1146/annurev-immunol-073119-095439
30. López-Casado MA, Lorite P, Palomeque T, Torres MI. Potential role of the IL-33/ST2 axis in celiac disease. Cell Mol Immunol. 2017;14(3):285-292. doi:10.1038/cmi.2015.85
31. Perez F, Ruera CN, Miculan E, et al. IL-33 Alarmin and Its Active Proinflammatory Fragments Are Released in Small Intestine in Celiac Disease. Front Immunol. 2020;11(October):1-15. doi:10.3389/fimmu.2020.581445
32. Manti S, Cuppari C, Tardino L, et al. HMGB1 as a new biomarker of celiac disease in children: A multicenter study. Nutrition. 2017;37:18-21. doi:10.1016/j.nut.2016.12.011
33. Manavalan JS, Hernandez L, Shah JG, et al. Serum cytokine elevations in celiac disease: Association with disease presentation. Hum Immunol. 2010;71(1):50-57. doi:10.1016/j.humimm.2009.09.351
34. Palone F, Vitali R, Trovato CM, et al. Faecal high mobility group box 1 in children with celiac disease: A pilot study. Dig liver Dis Off J Ital Soc Gastroenterol Ital Assoc Study Liver. 2018;50(9):916-919. doi:10.1016/j.dld.2018.04.003
35. Herrera MG, Gómez Castro MF, Prieto E, et al. Structural conformation and self-assembly process of p31-43 gliadin peptide in aqueous solution. Implications for celiac disease. FEBS J. Published online 2019. doi:10.1111/febs.15109
36. Ruera CN, Miculan E, Ducca G et al. IL-1β blockade prevents cell death and mucosal damage of the small intestine in a model of sterile inflammation. immunol Letters. 5, 248–253 (2022). doi: 10.1016/j.imlet.2022.10.006
37. Porpora M, Conte M, Lania G, et al. Inflammation Is Present, Persistent and More Sensitive to Proinflammatory Triggers in Celiac Disease Enterocytes. Int J Mol Sci. 2022;23(4). doi:10.3390/ijms23041973
38. Lamkanfi M, Dixit VM. Mechanisms and functions of inflammasomes. Cell. 2014;157(5):1013-1022. doi:10.1016/j.cell.2014.04.007
39. Günther C, Martini E, Wittkopf N, et al. Caspase-8 regulates TNF-α-induced epithelial necroptosis and terminal ileitis. Nature. 2011;477(7364):335-339. doi:10.1038/nature10400
40. Lee SH, Kwon JY, Moon J, et al. Inhibition of RIPK3 pathway attenuates intestinal inflammation and cell death of inflammatory bowedisease and suppresses necroptosis in peripheral mononuclear cells of ulcerative colitis patients. Immune Netw. 2020;20(2):1-15. doi:10.4110/in.2020.20.e16
41. Teh CE, Preston SP, Robbins AK, et al. Caspase-8 has dual roles in regulatory T cell homeostasis balancing immunity to infection and collateral inflammatory damage. Sci Immunol. 2022;7(69):eabn8041. doi:10.1126/sciimmunol.abn8041
42. Bayardo M, Punzi F, Bondar C, Chopita N, Chirdo F. Transglutaminase 2 expression is enhanced synergistically by interferon-γ and tumour necrosis factor-α in human small intestine. Clin Exp Immunol. 2012;168(1):95-104. doi:10.1111/j.1365-2249.2011.04545.x
43. Woznicki JA, Saini N, Flood P, et al. TNF-α synergises with IFN-γ to induce caspase-8-JAK1/2-STAT1-dependent death of intestinal epithelial cells. Cell Death Dis 2021 1210. 2021;12(10):1-15. doi:10.1038/s41419-021-04151-3
44. Di Sabatino A, Miceli E, Dhaliwal W, et al. Distribution, proliferation, and function of paneth cells in uncomplicated and complicated adult celiac disease. Am J Clin Pathol. 2008;130(1):34-42. doi:10.1309/5ADNAR4VN11TTKQ6
45. Pandian, Nagakannan y Thirumala-Devi Kanneganti. " PANoptosis: A Unique Innate Immune Inflammatory Cell Death Modality.". The Journal of Immunology 209 (2022): 1625 - 1633. doi: 10.4049/jimmunol.2200508.
46. Schwarzer R, Laurien L, Pasparakis M. New insights into the regulation of apoptosis, necroptosis, and pyroptosis by receptor interacting protein kinase 1 and caspase-8. Curr Opin Cell Biol. 2020;63:186-193. doi:10.1016/j.ceb.2020.02.004
47. Karki R, Sharma BR, Lee E, et al. Interferon regulatory factor 1 regulates PANoptosis to prevent colorectal cancer. JCI Insight. 2020;5(12). doi:10.1172/jci.insight.136720
48. Romero-Garmendia I, Garcia-Etxebarria K, Hernandez-Vargas H, et al. Transcription factor binding site enrichment analysis in co-expression modules in celiac disease. Genes (Basel). 2018;9(5):1-12. doi:10.3390/genes9050245
49. Chaouhan HS, Vinod C, Mahapatra N, et al. Necroptosis: A Pathogenic Negotiator in Human Diseases. International Journal of Molecular Sciences. 2022; 23(21):12714. https://doi.org/10.3390/ijms232112714
50. Günther C, Ruder B, Stolzer I et al. Interferon Lambda Promotes Paneth Cell Death Via STAT1 Signaling in Mice and Is Increased in Inflamed Ileal Tissues of Patients With Crohn's Disease. Gastroenterology. 2019 Nov;157(5):1310-1322.e13. doi: 10.1053/j.gastro.2019.07.031.
51. Xu S, He Y, Lin L et al. The emerging role of ferroptosis in intestinal disease. Cell Death Dis. 2021 Mar 17;12(4):289. doi: 10.1038/s41419-021-03559-1.

Acknowledgments
We thank Allan McI. Mowat for his helpful comments and critical reading of this manuscript.

Ethical approval
The study was approved by the Ethical Committees of both Public Health Institutions and performed according to human experimental guidelines. The clinical investigation was conducted according to the Declaration of Helsinki principles with participants identified only by number.

Funding
This work was supported by grants PICT-2017- 0880 (2019-2022) and PICT-2020- SERIE A-00434 (2022-2024) from the Agencia Nacional de Promoción Científica y Tecnológica, Ministerio de Ciencia, Tecnología e Innovación Productiva, and CONICET PIP 2021. 11220200102374CO (2021-2023), República Argentina. The founders had no role in study design, data collection, and analysis, or the decision to publish or preparation of the manuscript.

Conflicts of interest
Authors declare no conflict of interest

Data availability
The data underlying this article are available in the article and in its online supplementary material.

Author contributions
CR acquired data, analyzed and interpreted data, and wrote the manuscript. CR, FP, and MLI collected and processed the human samples. FP performed the gene analysis from datasets. LaG, LuG, and LM performed the clinical evaluation and endoscopy procedures. FCh designed the research, analyzed data, and wrote the manuscript.

Permission to reproduce
Not applicable.

Trial registration

Not applicable.

Figure legends

Figure 1. Cell death in the duodenal mucosa during celiac disease. **(A).** Representative images of TUNEL staining of duodenal sections from ACD patients and NC. DAPI staining for nuclei (blue), TUNEL$^+$ cells (green). (**B).** TUNEL$^+$ cells density in *lamina propria* of individual patients. Data are expressed as the number of TUNEL$^+$ cells per µm^2 of *lamina propria* ± 1 SEM. (NC= 6, ACD= 8). *****P<0.0001*. Student's unpaired t-test with Welch correction.

Figure 2. Characterization of TUNEL$^+$ *lamina propria* cells in active celiac disease. **(A).** Representative images of TUNEL staining and lineage markers in duodenal sections from ACD patients. IP staining for nuclei (blue), TUNEL$^+$ cells (green), and lineage markers (CD45, CD138, CD3) (red). White arrows indicate double positive cells for each marker and dotted arrows indicate TUNEL$^+$ cells close to CD3$^+$ cells (**B).** Double-positive cells density in *lamina propria* of duodenal sections. Data are expressed as the % of total TUNEL$^+$ cells expressing each marker ± 1 SEM. (CD45 n=5, CD138 n=5, CD20 n=7, CD64 n=3, CD3 n=7; the "n" in each plot corresponds to the number of ACD patients used to calculate the % of TUNEL$^+$ cells per cell type) **(C).** Left: Representative images of TUNEL and CD3 staining in ACD patients. Nuclei (blue), TUNEL$^+$ cells (green), CD3 (red) Right: Zoom of a representative image of TUNEL$^+$ cells in ACD in close contact with CD3$^+$ T cells. dotted arrows indicate TUNEL$^+$ cells close to CD3$^+$ cells **(D)** Representative images of TUNEL, CD3 and CD95 staining. Nuclei (blue), TUNEL$^+$ cells (green), CD3 (red), and CD95 (violet). White arrows indicate the same cells with stainings for different markers associated with T cell-mediated cytotoxicity by the Fas/FasL axis.

Figure 3. Expression of cleaved caspase-8 and -3 in duodenal mucosa of active celiac disease. (A). Representative immunofluorescent staining for expression of caspase-8 (top) and caspase-3 (bottom) in duodenal mucosa of NC and ACD patients. Caspase-8 and -3 (red), Nuclei (blue). **(B).** Representative Western blots for pro- and cleaved caspase-8 and -3, with β-actin as the loading control. (**C).** Top: Quantitative analysis of Western blot bands expressed as the ratio of cleaved caspase-8:procaspase-8 in NC (n=8) or ACD (n=12) patients. ***P<0.01*; Student's unpaired t-test. Bottom: Quantitative analysis of Western blot bands expressed as the ratio of cleaved caspase-3:procaspase-3 in NC (n=12) or ACD (n=12) patients. ****P<0.001*; Student's unpaired t-test.

Figure 4. Expression of inflammasome proteins in duodenal mucosa of active celiac disease. (A). Representative immunofluorescent staining for expression of caspase-1 (top), GSDMD (center), and IL-1β (bottom) in duodenal mucosa of NC and ACD patients. Caspase-1, GSDMD and IL-1β (red), Nuclei (blue). **(B).** Representative Western blots for pro- and cleaved caspase-1 (top), intact and N-terminal GSDMD (center), and mature IL-1β (bottom), with β-actin as the loading control protein. **(C).** Quantitative analysis of Western blot bands, showing top: ratio of cleaved caspase-1:procaspase-1 in NC (n=8) or ACD (n=8). ***P<0.01*; Student's unpaired t-test with Welch correction. Center: ratio of N-terminal:Full GSDMD in NC (n=4) or ACD (n=4) patients. **P<0.05*; Student's unpaired t-test. Bottom: ratio of mature IL-1β: β-actin in NC (n=7) and ACD (n=7) patients. ****P<0.001*; Student's unpaired t-test with Welch correction.

Figure 5. Necroptosis in the duodenal mucosa of active celiac disease. (A). Representative immunofluorescent staining for RIPK3 expression in duodenal mucosa of NC and ACD patients. RIPK3 (red), nuclei (blue). (**B).** Left: Representative Western blots for RIPK3 in NC and ACD patients, with β-actin as the loading control protein. Right: Quantitative analysis of Western blot bands expressed as the ratio of RIPK3: β-actin in NC (n=6) and ACD (n=6) patients. *ns, P=0.06*; Student's unpaired t-test

with Welch correction. (**C).** Left: Representative Western blots for p-MLKL in NC and ACD patients with β-actin as the loading control protein. Right: Quantitative analysis of Western blot bands expressed as the ratio of p-MLKL: β-actin in NC (n=5) and ACD (n=9) patients. **P<0.05*; Student's unpaired t-test with Welch correction. (**D).** Co-localization of p-MLKL with Paneth cells (α-defensin 5^+), and $CD3^+$ T lymphocytes in duodenal biopsies from ACD patients. Representative immunofluorescent staining for co-expression of p-MLKL with α-defensin 5 (**top**), and CD3 with p-MLKL (**bottom**). Nuclei (blue), p-MLKL (red), CD3 or DEFA5 (green). White arrows indicate double positive cells. **(E-F).** Dot plots showing RT-qPCR results for expression of mRNA for MLKL (NC=5, ACD= 9) (**E**) and ZBP1 (NC=5, ACD= 8) (**F**). Results show levels of mRNA expressed as a ratio to levels of the EEF1A1 housekeeping gene and are means ± SEM. **P<0.05*, ***P<0.01*; Student's unpaired t test.

Figure 6. Transcriptomic analysis of regulated cell death-related genes in celiac disease. (A). Heatmap showing scaled DEGs related to apoptosis, pyroptosis, and necroptosis from a public database of 24 CD and 21 non-CD (control) patients (GSE164883). Dendrograms on the left sort DEGs based on their pattern of expression across patients and the color scale shows the mean z-score. (**B).** Heatmap showing the mean scaled expression of DEGs related to RCDs from a public database derived from scRNA-seq analysis of plasma cells sorted from 15 patients with untreated CD (UCD), 26 gluten-free diet treated CD (TCD) and 13 non-CD patients (healthy) (EGAS00001004623). The dendrogram at the top sorts the three evaluated cohorts based on the similarity of the expression pattern of DEGs. The color scale shows the mean z-score.

Figure 1

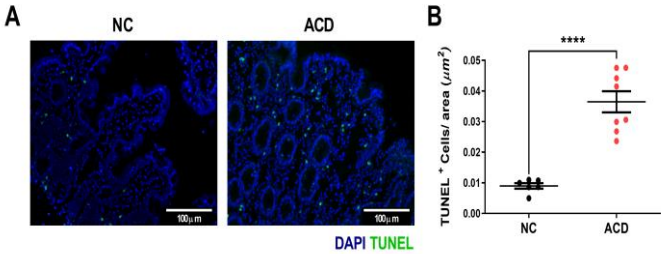

Figure 2

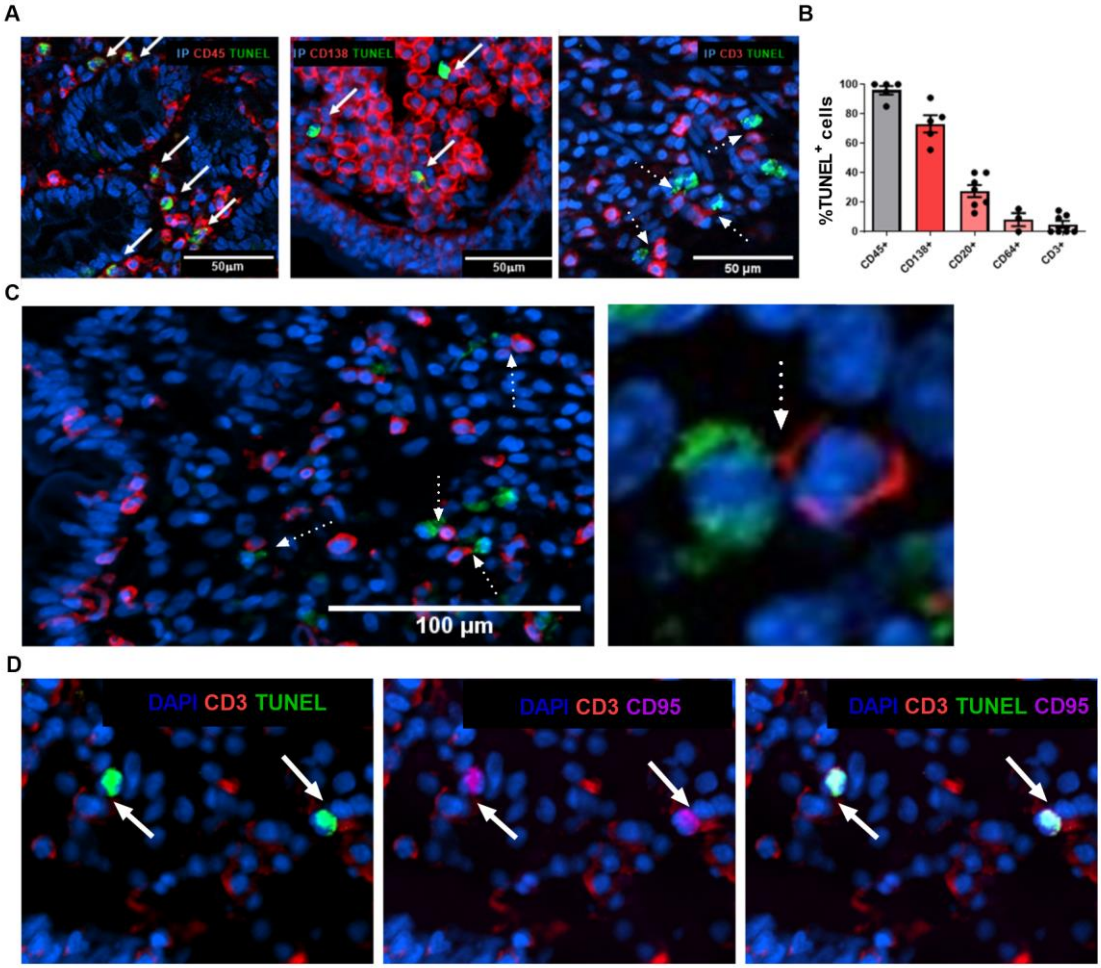

Figure 3

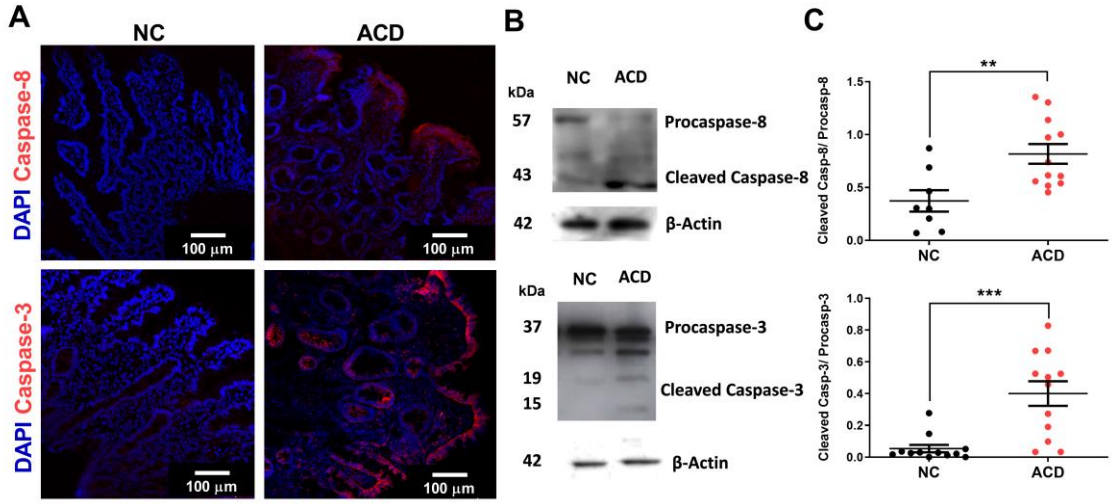

Figure 4

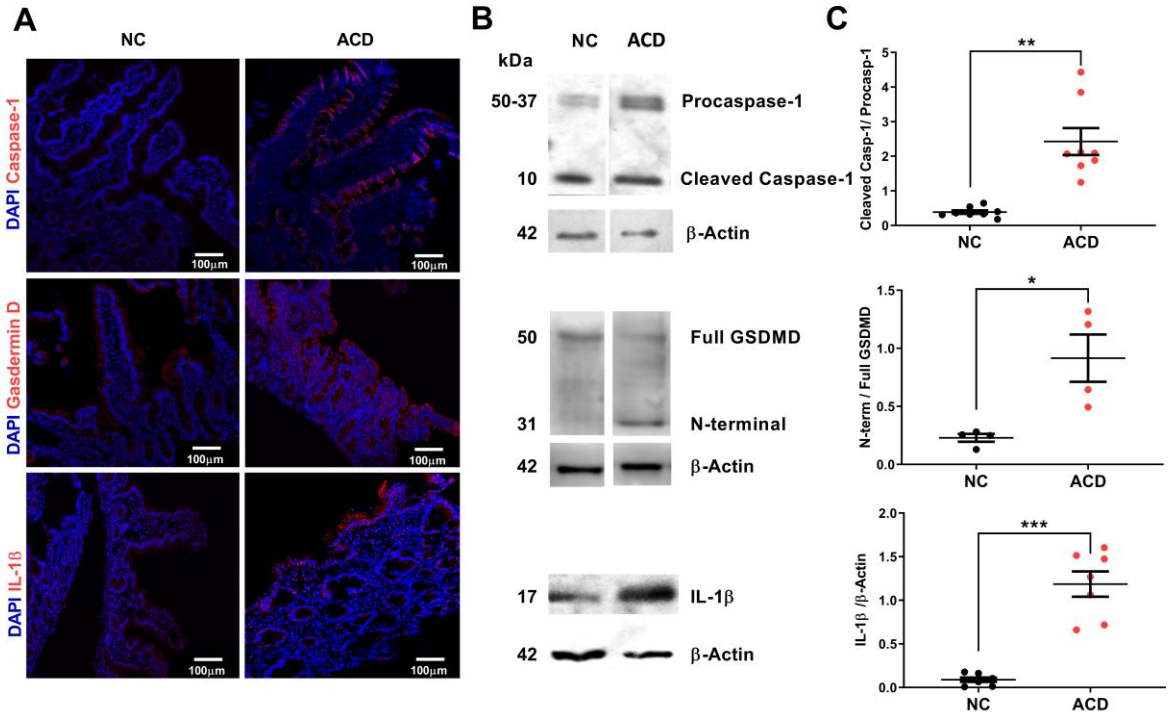

Figure 5

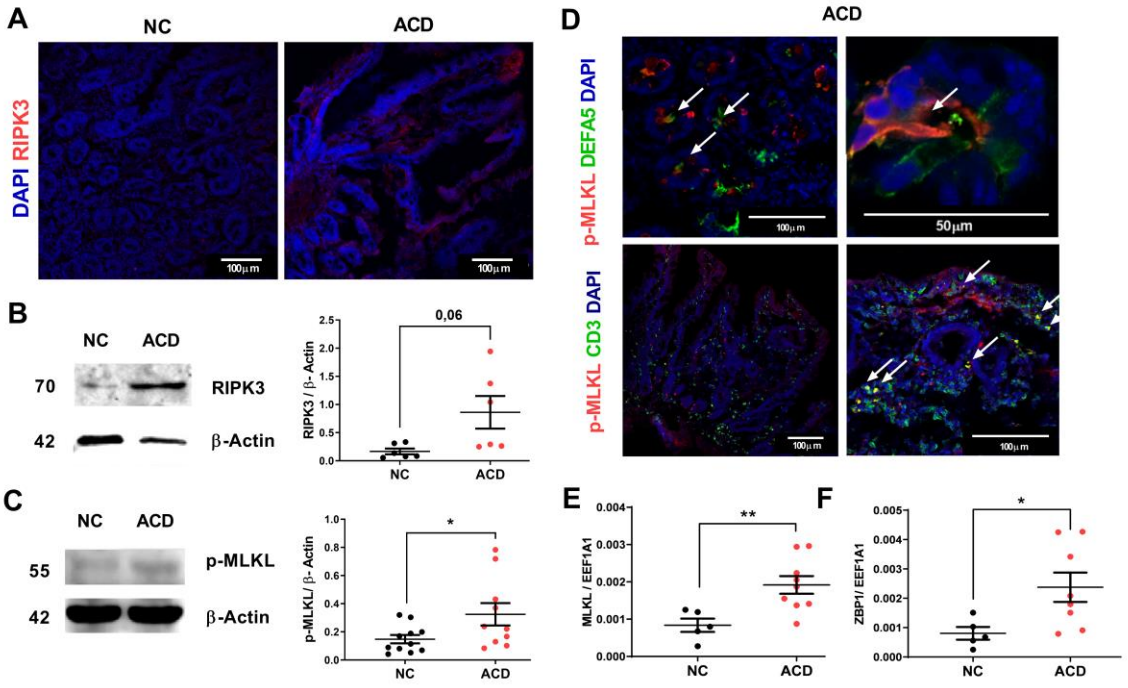

Figure 6